

# Factors Limiting Performance of CdZnTe Detectors

Aleksey Bolotnikov

Detector Development and Testing Division  
Nonproliferation and National Security  
Upton, NY 11793 USA

Thanks to

Gomez Wright  
Gabriella Carini  
Giuseppe Camarda

Peter Siddons

Ralph James

## Comparison CdZnTe & HPGGe:

### Two problems

Small crystal size:  
typically  $< 1 \text{ cm}^3$

Poor charge collection:  
holes trapped instantly;  
Electron lifetime  $\sim 1.5\text{-}2.5 \text{ us}$   
or  $\sim 2 \text{ cm}$  drift length at  
 $E=100 \text{ V/mm}$

### Two great advantages

Can operate at room  
temperature: between  
 $-30$  and  $30 \text{ C}$

High stopping power:  
CZT:  $Z\sim 50, D\sim 5.9 \text{ g/cm}^3$   
Ge:  $Z\sim 32, D\sim 5.3 \text{ g/cm}^3$

These makes CZT material very attractive but it requires  
special detector designs:

Using arrays of  
CZT detectors.

Single carrier devices:  
pixel, coplanar-grid,  
virtual-Frisch-grid, etc.

Charge loss correction  
techniques: rise time  
(depth) correction, detector  
segmentation, etc.

Among many factors determining  
performance of CZT detectors there are  
several which are common:

- Bulk and surface conductivity
- Fluctuation of electron loss due to trapping.
- Device geometry.

## I. Bulk and surface leakage current

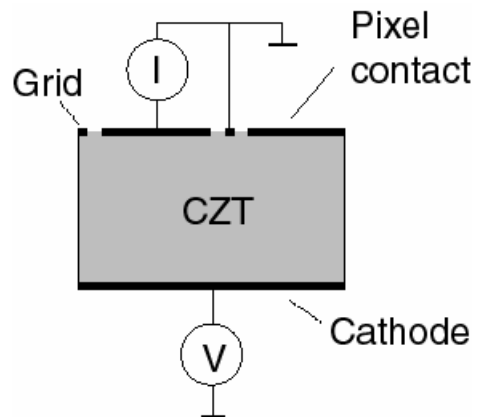
Why it is important:

- leakage current directly contributes to electronic noise and affect energy resolution
- surface conductivity affects charge collection in multi-electrode devices such as pixel, coplanar-grid, Frisch-grid, etc.

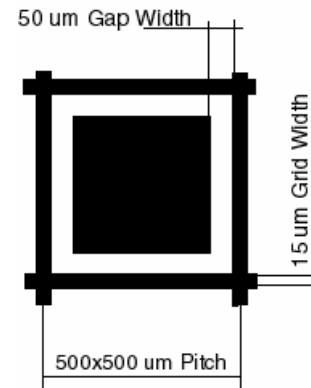
Most of the vendors fabricate CZT detectors with Pt or Au contacts (accept Imarad). The results presented here were obtained with these types of detectors.

## Bulk leakage current measurements

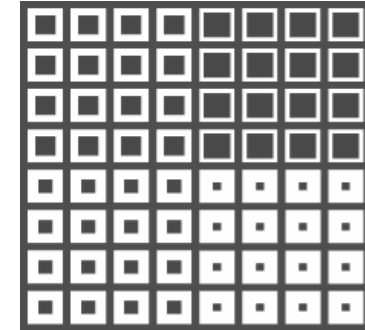
Details in NIM 482, p. 395, 2002.



- Keithley SourceMeter
- D.C calibrator
- GPIB controlled



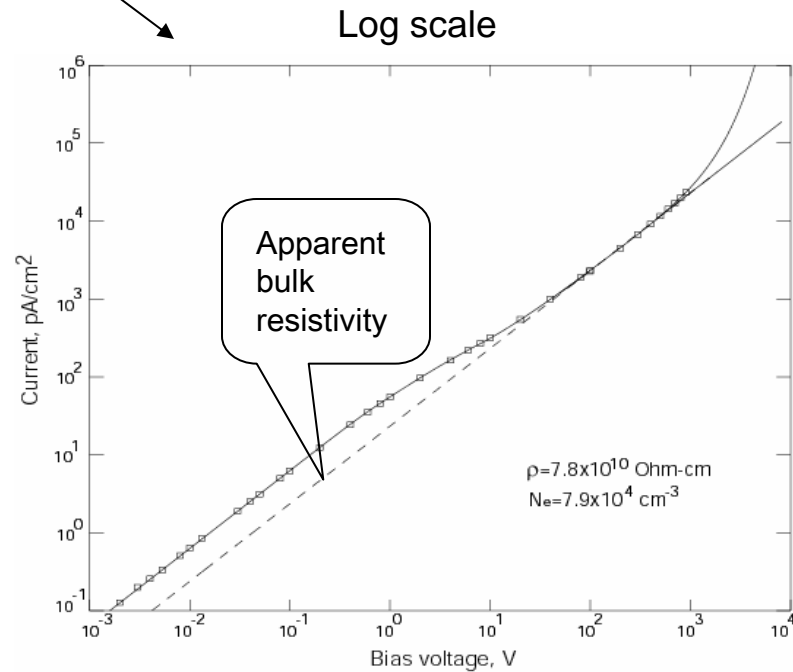
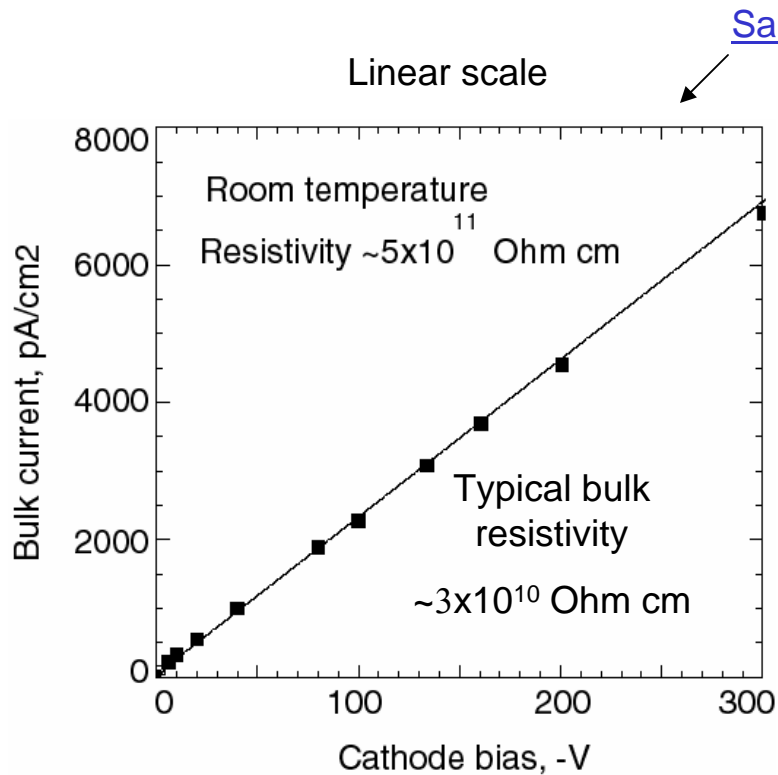
Pixel contact surrounded by grid is most suitable



### Important requirements

- grid is grounded (to provide uniform field inside CZT and intercept surface current)
- take measurements at steady state current condition
- temperature monitoring (results very sensitive to temperature variations)
- take measurements in wide range of biases: 0.001-1000 V

## Example of data misinterpretation

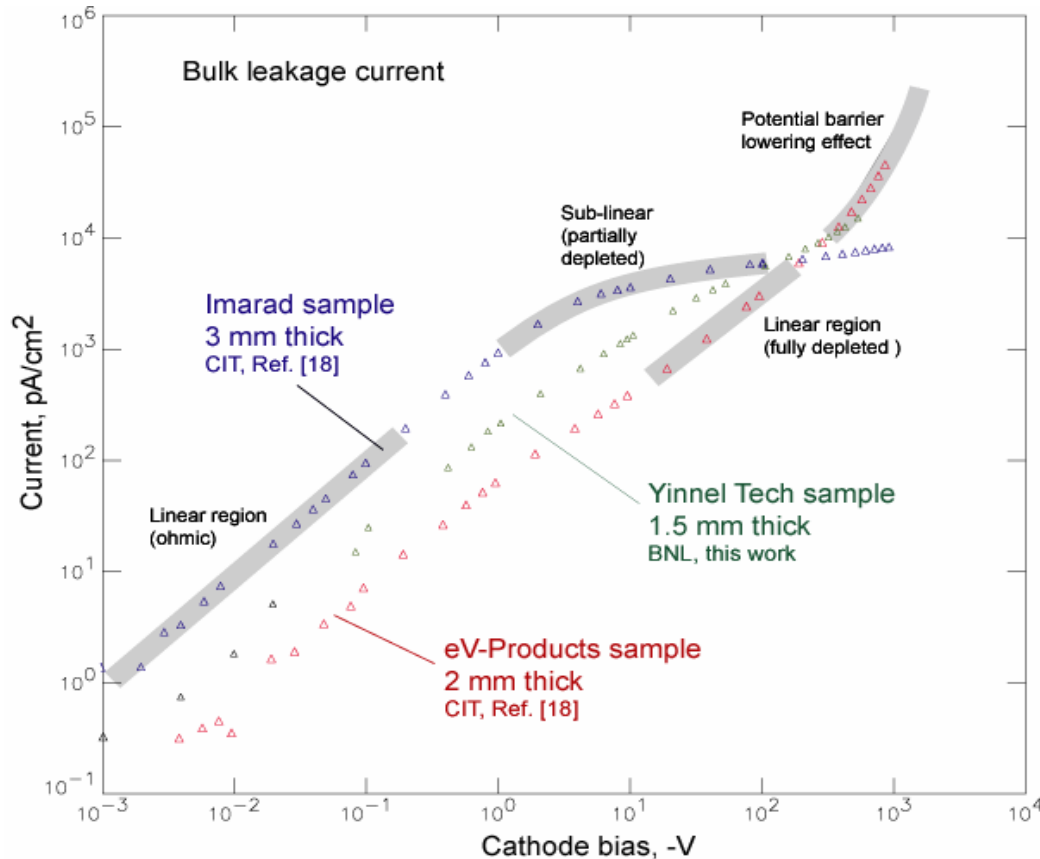


This example shows how easy to make an error !

*I-V* curve has two linear regions:

- (1) true ohmic behavior;
- (2) so-called diffusion-limited current. It resembles ohmic law but with very high “effective” bulk resistivity

## Typical I-V curves measured with detectors fabricated by different vendors



Four distinguish regions in I-V curve:

- (1) Ohmic, or bulk resistivity limited current.
- (2) Sub-linear
- (3) Linear
- (4) Exponential rise

Fitting results:

$3 \times 10^9$  Ohm-cm – Imarad

$5 \times 10^{10}$  Ohm-cm – eV-Products

$3 \times 10^{10}$  Ohm-cm – Yinnel Tech

but... ~200-400 V leakage currents are the same!

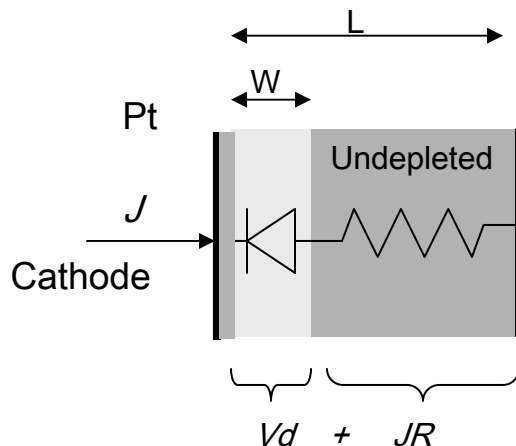
Such behavior can be understood if consider CZT device as metal-semiconductor-metal (MSM) system with two back-to-back Schottky barrier contacts

## Application of Schottky barrier model to CZT detector

Two additional features:

- High bulk resistivity.
- Interfacial layer => potential barrier lowering effect

CZT detector can be modeled a represent reverses biased diode Schottky barriers and resistor that represents undepleted bulk



According to **interfacial layer-thermionic-diffusion** theory for the Schottky-barrier diode (Wu, J. Appl. Phys. 53, pp. 5947-5950, 1982), the reverse current across the diode is:

$$J = \mathcal{G}A^*T^2 f(Ec) \exp(-\Phi/kT) \times (1 - \exp\{-(V-RJ)/kT\}),$$

$A^*$  is Richardson constant,  $T$  is temperature,  $\mathcal{G}$  is transmission coefficient through interfacial layer,  $R$  is bulk resistance,  $Ec$  is electric field strength near contact,  $\Phi$  is effective potential barrier,  $f(Ec)$  is a function of that can be calculated numerically.

Potential barrier lowering effect due to interfacial layer (simplest approach):

$$\Phi = \Phi_0 - \beta V,$$

where  $\Phi_0$  is a potential barrier at zero bias.

Dependence  $Ec(V, W, Vdep)$  can be calculated based on Schottky depletion model and assuming concentration of ionized levels  $N_D$ . Additional equations for resistance of undepleted layer and voltage drop across diode:

$$R = (L - W) / eN_D\mu,$$

$$V + V_{bi} = (eN_D / 2\epsilon) W^2 + JR$$

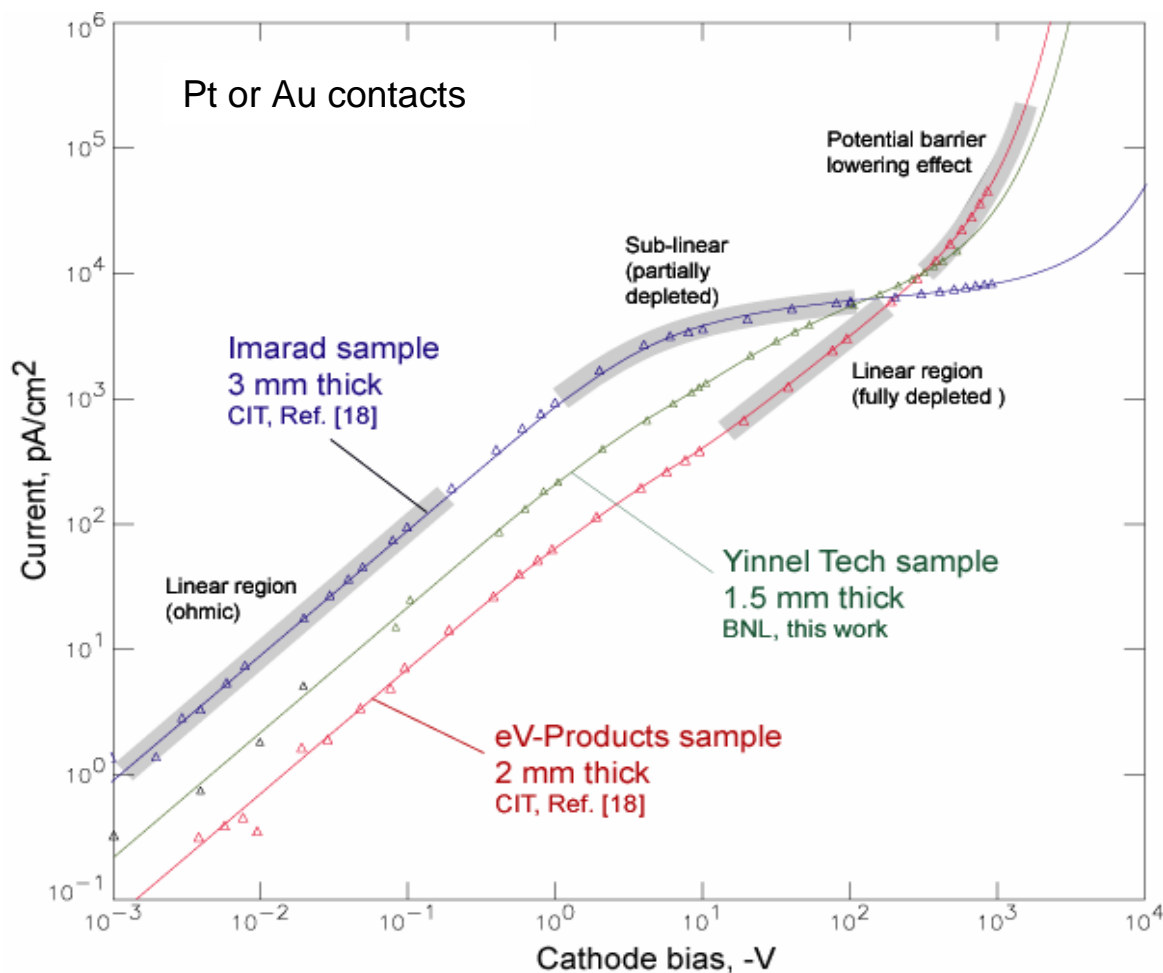
$J$  and  $W$  can be found by solving above equations.

Free (fitting) parameters:  $n$ ,  $N_D$ ,  $\Phi_0$ ,  $\beta$ ,  $\mathcal{G}$ ,  $Vdep$

Known parameters:  $A^*$ ,  $\mu$

Details in NIM 482, p. 395, 2002.

## Typical I-V curves measured with detectors fabricated by different vendors



### Fitting results

#### Bulk resistivity:

3x10<sup>9</sup> Ohm-cm – Imarad

5x10<sup>10</sup> Ohm-cm – eV-Products

3x10<sup>10</sup> Ohm-cm – Yinnel Tech

#### Bias required to deplete CZT

4.5 V (eV-Products)

7.5 V (Yinnel Tech)

360 V (Imarad) => Indium contacts!

#### Potential barrier height:

0.740 eV (Imarad)

0.784 eV (eV-Products)

0.810 eV (Yinnel Tech)

These results are in good agreement with photovoltaic measurements by E.J. Morton et al., Nucl. Instr. and Meth., A 458 (2001) 558-562

## Electronic properties of CZT in comparison with Si

### CdZnTe

- 1) CZT is “slow” semiconductor => **generalized theory** of Schottky barrier is to be applied
- 2) Very high bulk resistivity => resistance of undepleted layer cannot be neglected => dependence of the depletion layer cannot be described with simple analytical function:
- 3) Compensated semiconductor with high concentration of deep levels =>  $n < N_D$
- 4) Presence of interfacial layer between metal and semiconductor bulk => this affects potential barrier height. The exact mechanism of this is still unknown: dielectric layer like in MOS devices or p-n junction. Phenomenologically this reduction of potential barrier can be described as

$$\Phi = \Phi_0 - \beta V,$$

where  $\Phi_0$  is a potential barrier at zero bias.

### Si

- 1) “Fast” semiconductor; it has high mobility => current is described in **thermionic emission** approximation:

$$I = AT^2 \exp(-eV_0/kT) \times (\exp(eV/kT) - 1)$$

- 2) Resistance of undepleted part of semiconductor is neglected => dependence of the depletion layer can be described as:

$$W = (2\epsilon/eN_D)(V_{bi} - V - kT/e)$$

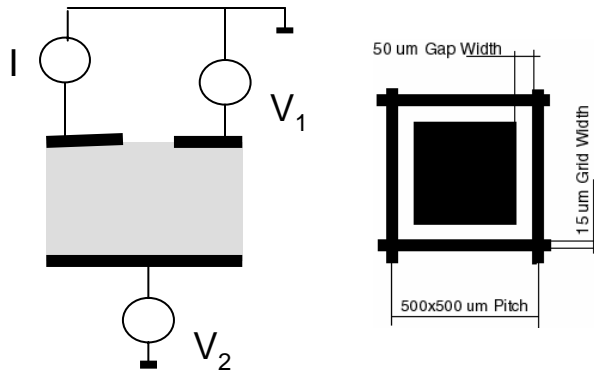
- 3) Free carrier concentration of bulk equals to the concentration of ionized states in depletion layer:

$$n = N_D$$

# Surface leakage current

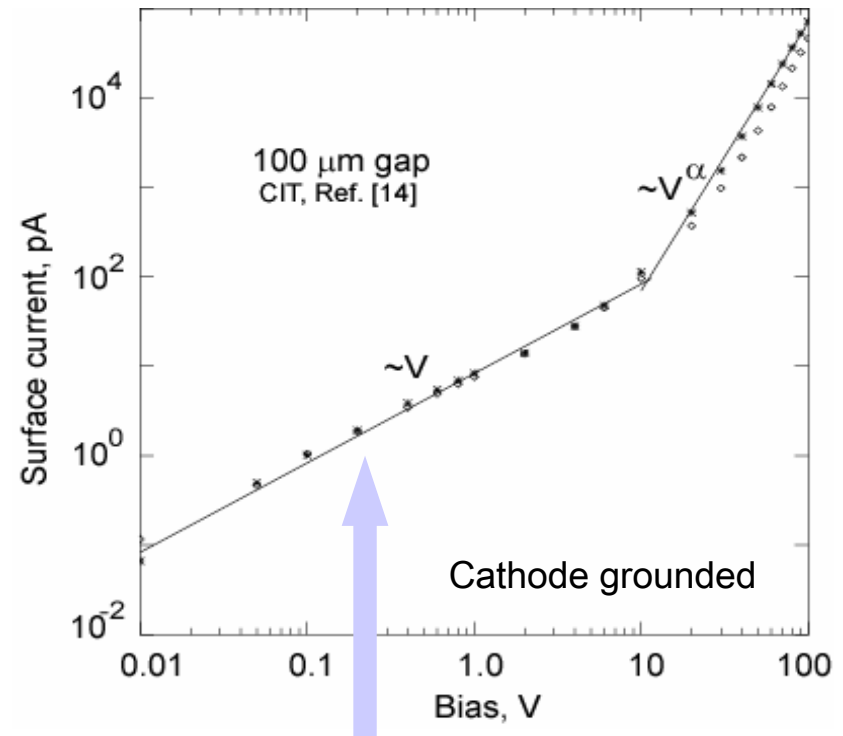
## Setup used for surface leakage current measurements

If gap is small bulk component can be neglected



- (1) Linear function of voltage (in first approximation)
- (2) Power law function,  $I \sim V^\alpha$ , with  $\alpha > 2$ . High-injection condition at the contact, but the current does not rise exponentially because the space charge limits injection.
- (3) Resistivity  $\sim 500$ - $5000$  GOhm/square

## Typical CZT sample (eV-Products )

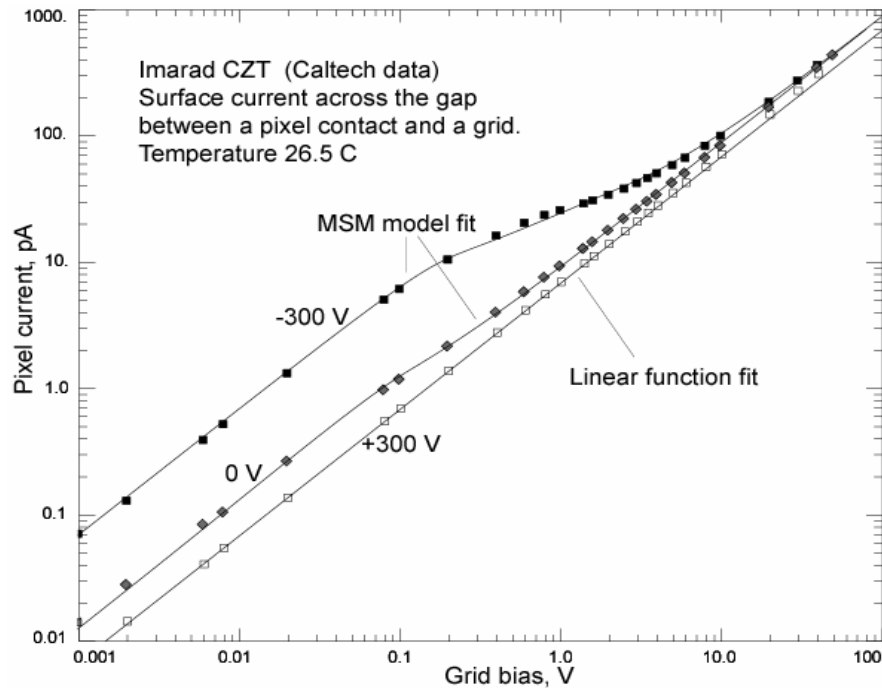


More accurate measurements revealed that this I-V is not linear in this region!

## Surface leakage current (more accurate measurements)

- 1) Current depends on cathode bias (field effect)
- 2) Surface I-V curves have similar shape as I-V curves measured for bulk

Data from NIM A510, p.300, 2003



If assume that current flows inside a thin surface layer, I-V curves can be fitted with the same MSM model that was used in the case of bulk currents.

### Fitting results for 50 nm thick layer:

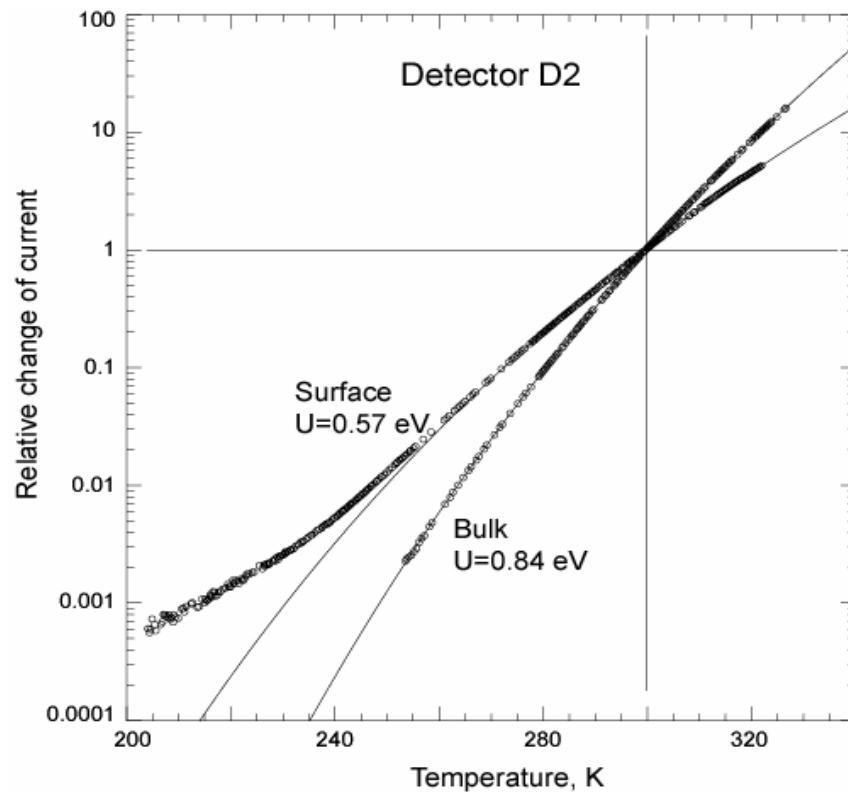
- barrier height  $\sim 0.51-0.53$  eV which is significantly less than for bulk
- carrier mobility  $\sim 100$  cm<sup>2</sup>/Vs (holes?)
- specific resistivity  $\sim 10^6-10^7$  Ohm-cm which is significantly less than for bulk.



Surface layer is a low resistivity  
p-type layer

## Temperature dependence of leakage currents

Data from NIM A510, p.300, 2003



Leakage currents rapidly drop with lowering temperature.

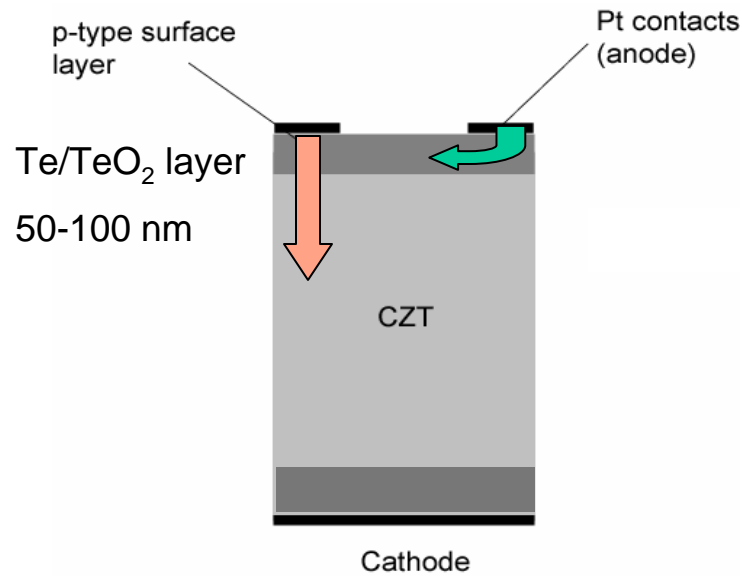
Use function  $\sim T^{3/2} \exp(-V/kT)$  to fit data (this function represents **diffusion limited** saturation current), where  $V$  is an effective barrier height.

$V$  found to be 0.57 and 0.84 eV for surface and bulk currents, respectively. These are very close to those obtained from bulk leakage current measurements.

# Properties of the surface layer

## Schematic of CZT device

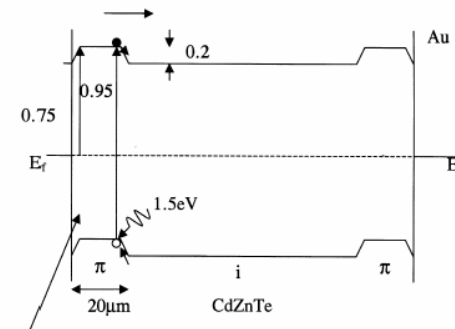
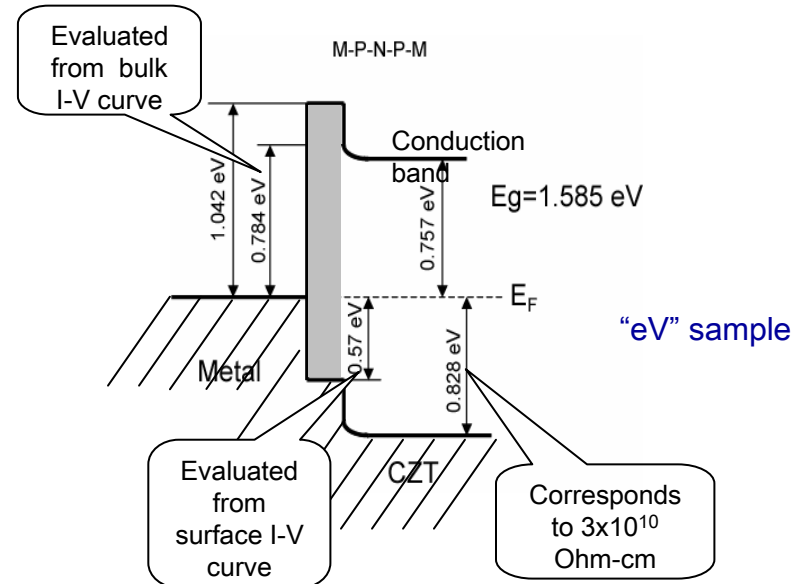
A. Rouse et al., *EEE Trans. Nucl. Sci.*, 2002. (eV-Products, Inc.)



Surface layer acts as a dielectric for electrons entering bulk CZT from contacts.

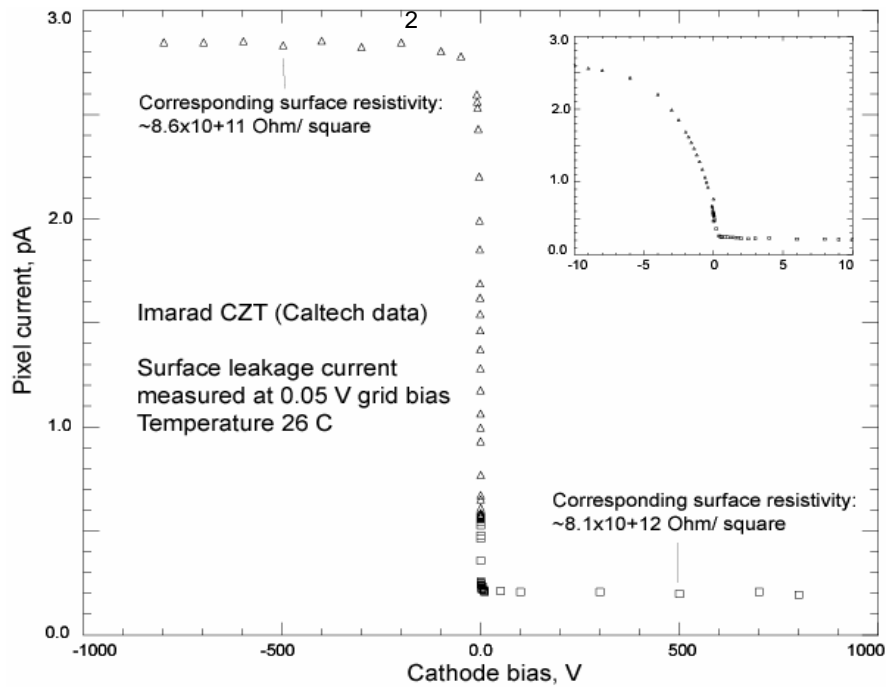
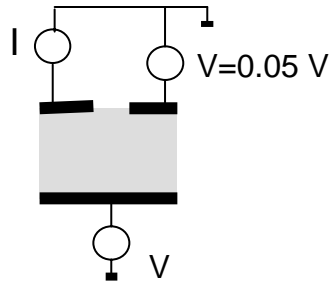
At the same time it serves as a low-resistivity conducting channel for holes.

## Device band structure: P-N-P



Photovoltaic measurements by E.J. Morton et al., *Nucl. Instr. and Meth.*, A 458 (2001) 558-562

## Field-effect



NIM A510, p.300, 2003)

Channel conductivity is enhanced at negative cathode bias => channel is p-type.

This is disappointing because negative bias is normally applied to the cathode.

At high bias the surface layer can be fully depleted regardless of the cathode bias.

However, at high bias, surface current becomes space charge limited.

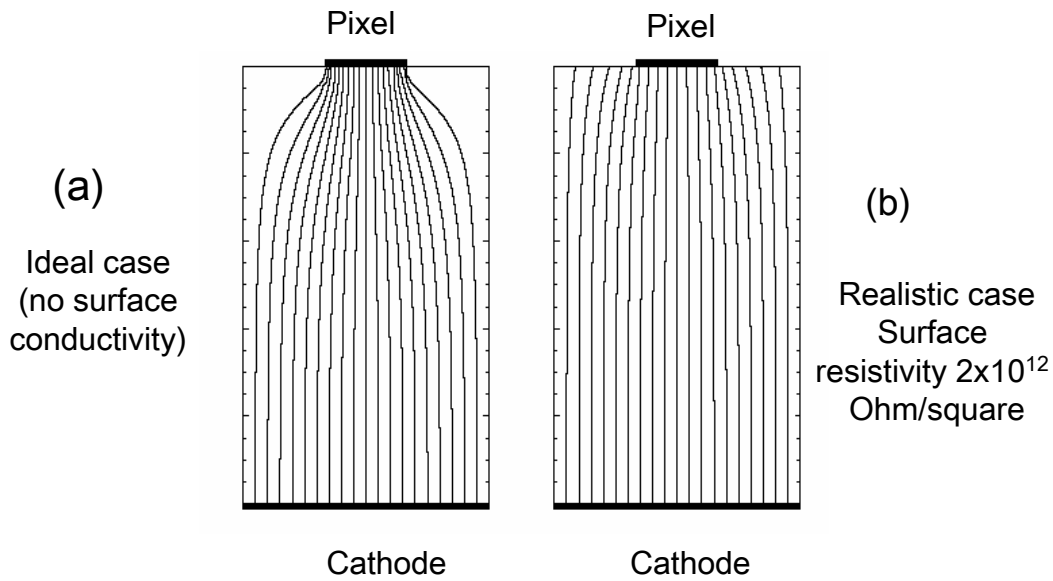
## Conclusions to bulk/surface leakage current effects

- actually measured bulk current is much smaller than the current calculated based on the bulk resistivity of CZT
- at high bias current rises exponentially if interfacial layer exists. It indicates if oxide layer was formed before making contacts
- typical bulk current ~ (5-10) pA at -300V for 400x400  $\mu\text{m}$  area and 2 mm thick CZT
- surface leakage current is located inside p-type surface layer, which can be depleted or enhanced like in a FET by changing cathode bias
- because of the field-effect the total leakage current is not always the sum of bulk and surface currents measured separately

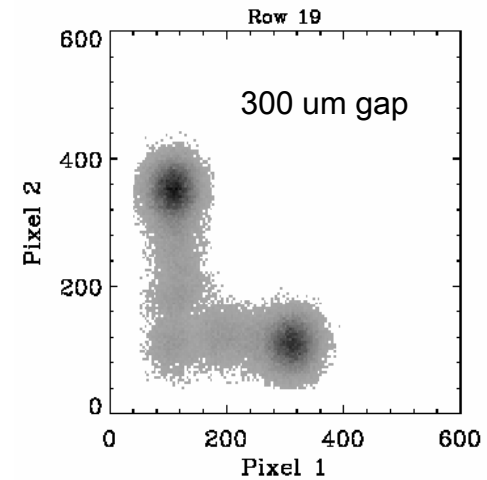
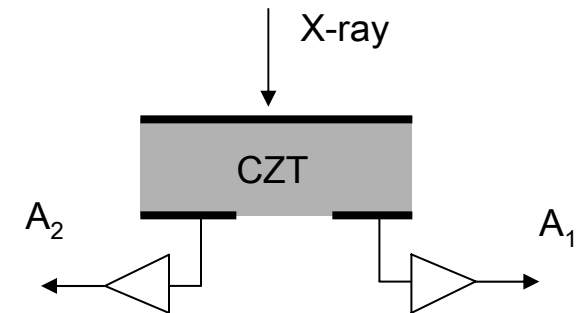
# Effects of surface conductivity on electric field (pixel device)

Caltech data (NIM, A432, p. 529, 1997)

200x200  $\mu\text{m}$  contact, 500  $\mu\text{m}$  pitch



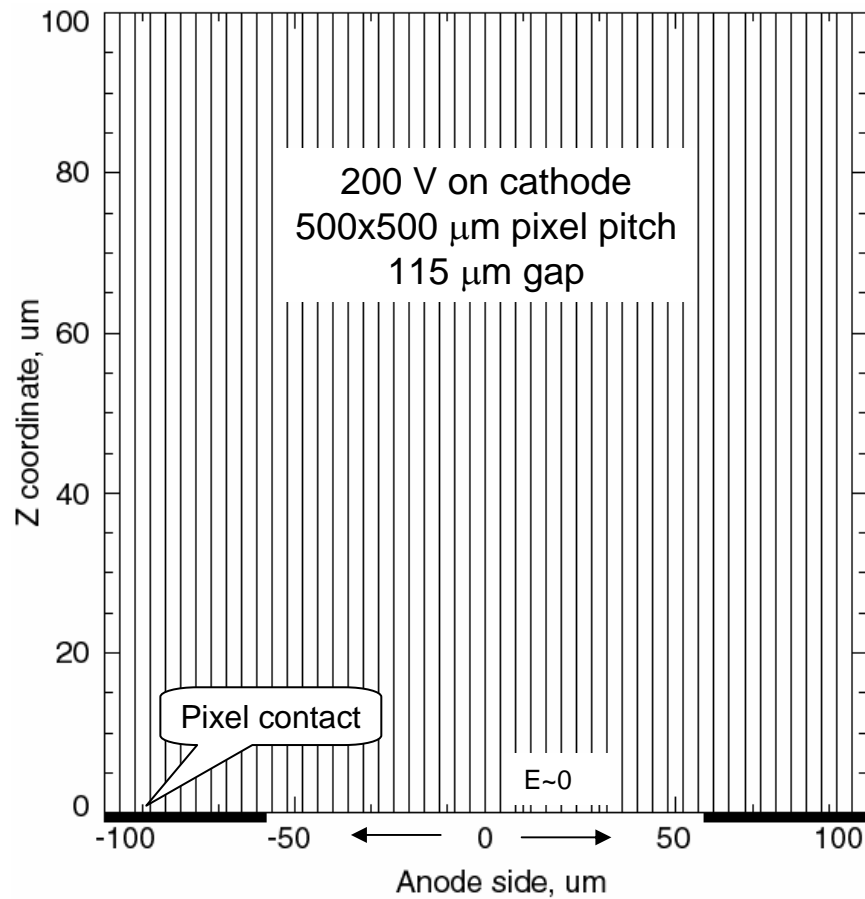
X-ray scan over two pixels



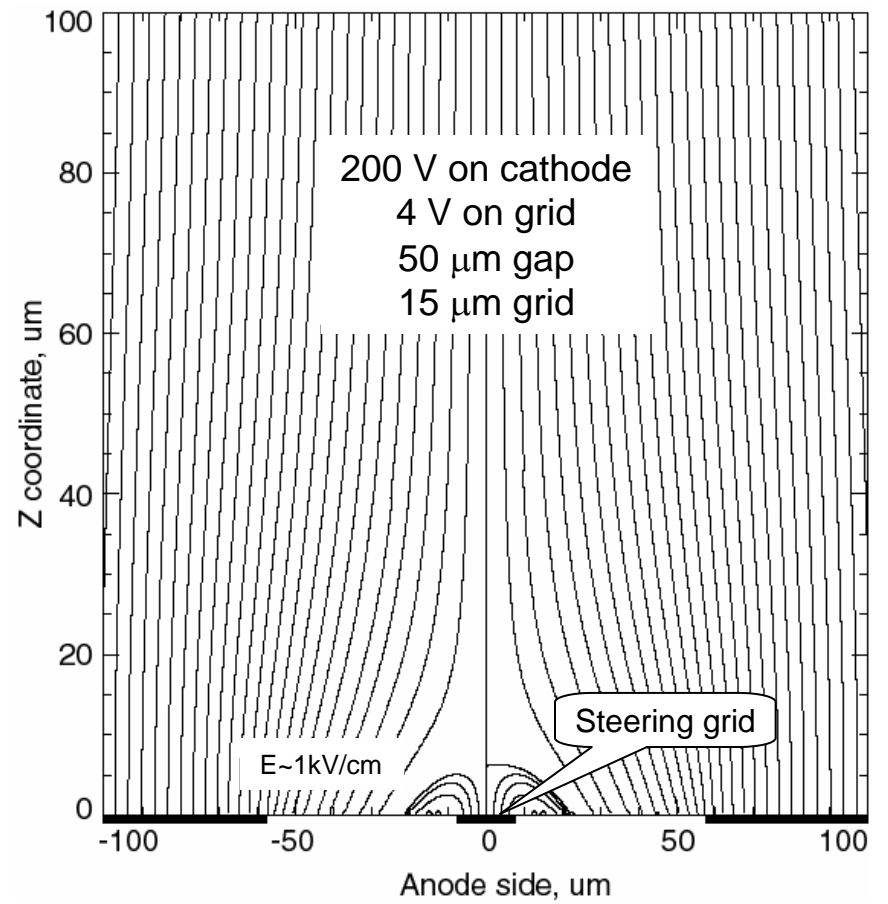
Solution of this problem is to use steering electrodes

## Electric field lines distribution inside CZT pixel detector

Pattern without steering grid

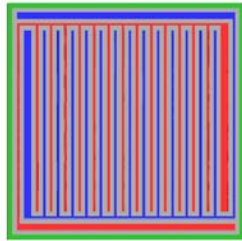


Pattern with steering grid



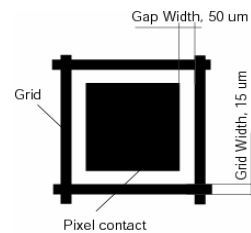
## Examples of devices with steering electrodes

### Coplanar-grid



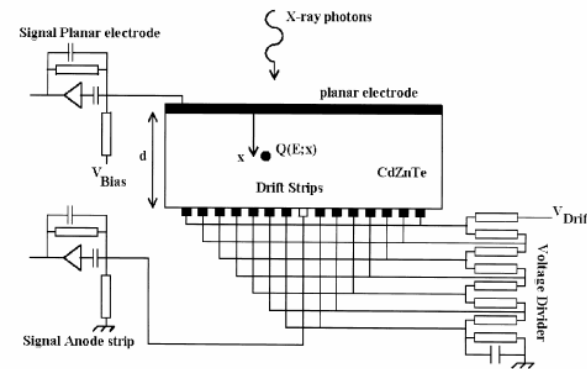
P. Luke

### Pixel detector with steering grid



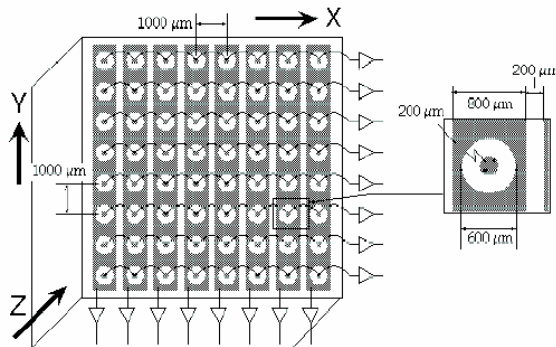
(CTI), SPIE, 2001

### Drift strip detector



(DSRI) C. Budtz-Jorgensen et al., NIM A 458 (2001) 132.

### Orthogonal Coplanar Anode Strip Detector



University of New Hampshire,  
J. M. Ryan et al. SPIE, 4851,  
2002.

Use of steering electrodes allows to reduce the size of the collecting electrodes.

However, it increases surface leakage current.

Space leakage current is usually space charge limited, by its nature, does not contribute significantly (but still contribute) to the electronic noise. This was experimentally shown by P. Luke

## Effects of surface conductivity in virtual Frisch-grid devices

Common feature of these devices is long side surfaces which may cause instabilities!

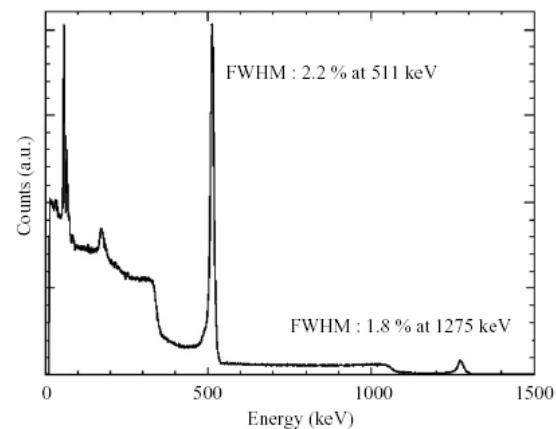
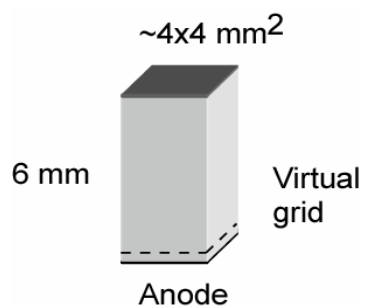
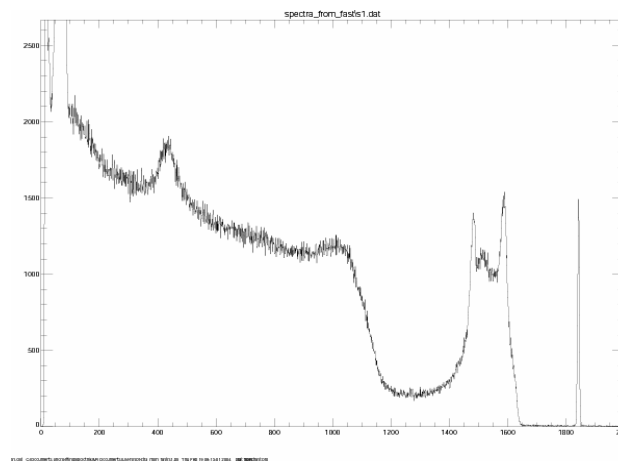
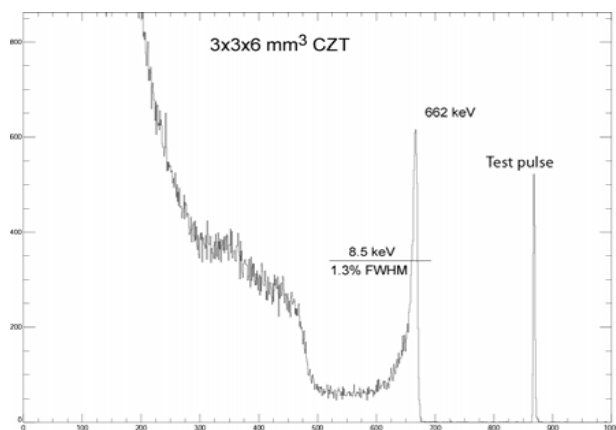


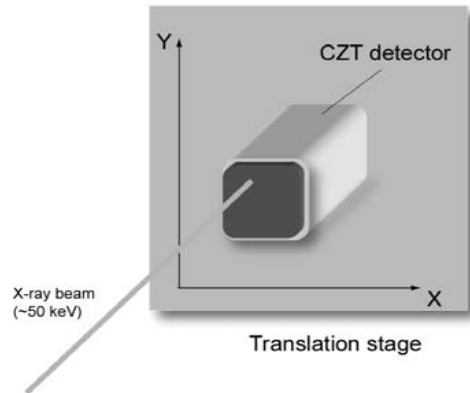
Fig. 13.  $^{22}\text{Na}$  spectrum recorded with a 6 mm thick CZT Capacitive Frisch Grid Structure at 21°C, 400 V.



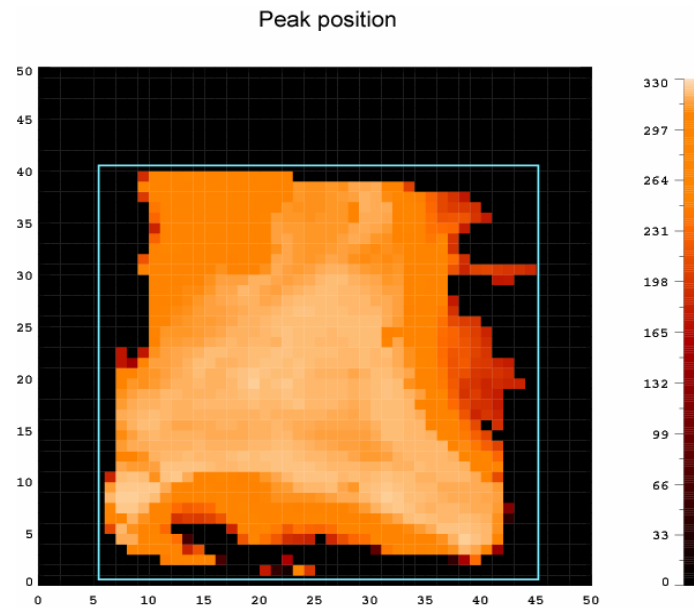
# X-ray scan of virtual Frisch-grid detector

Unique capabilities of National Synchrotron Light Source at BNL

X-ray beam characteristics:  
high intensity  
monochromatic  
focused down to 10x10  $\mu\text{m}$



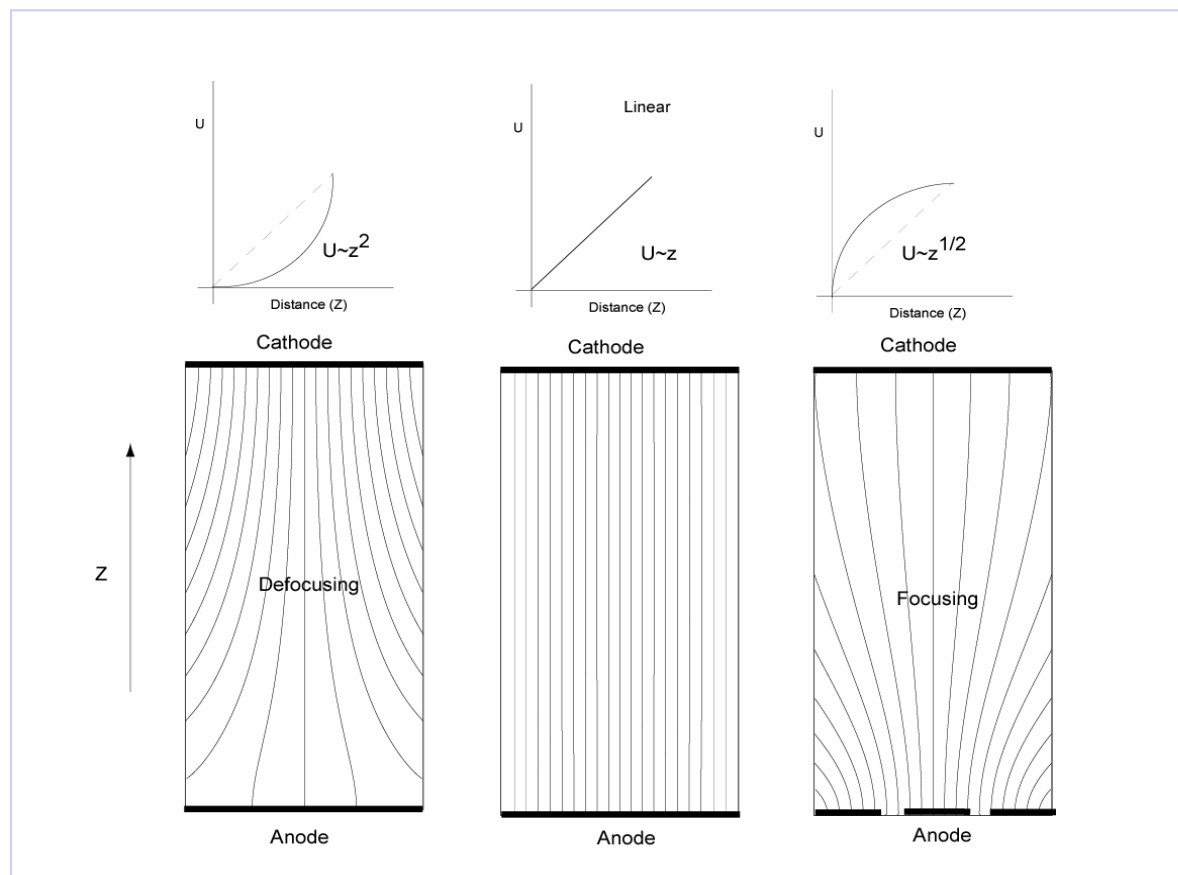
## Virtual Frisch-grid detector mapping



4x4x6 mm bar detector  
100 microns steps  
25x25 microns beam  
Cathode bias 800 V

## Calculated electric-field line distribution

Surface resistivity determines distribution of electrostatic potential along detector side surfaces and, thus, field lines distribution inside the detector



## II. Fluctuation of electron losses

It has been assumed for long time that charge loss due to trapping is a continues process that can be corrected. However, recent results indicate that electron trapping may introduce additional fluctuations caused by microscopic defects with high concentration of traps.

Such defects can trap large numbers of electrons in each interaction with an electron cloud. It is very natural to assume that number of trapped electrons fluctuates.

Possible candidates for such centers are inclusions, precipitates, or some other structural defects.

There are several facts that indicate an existence of such fluctuations.

# Experimental evidence of fluctuations of charge loss in long-drift detectors

1) Statistical limit was never achieved with detectors in which electrons travel long distances (**long-drift detectors**): coplanar-grid, virtual-grid, spherical, etc. Typical resolution obtained with such detectors is about 2-3% at 662 keV.

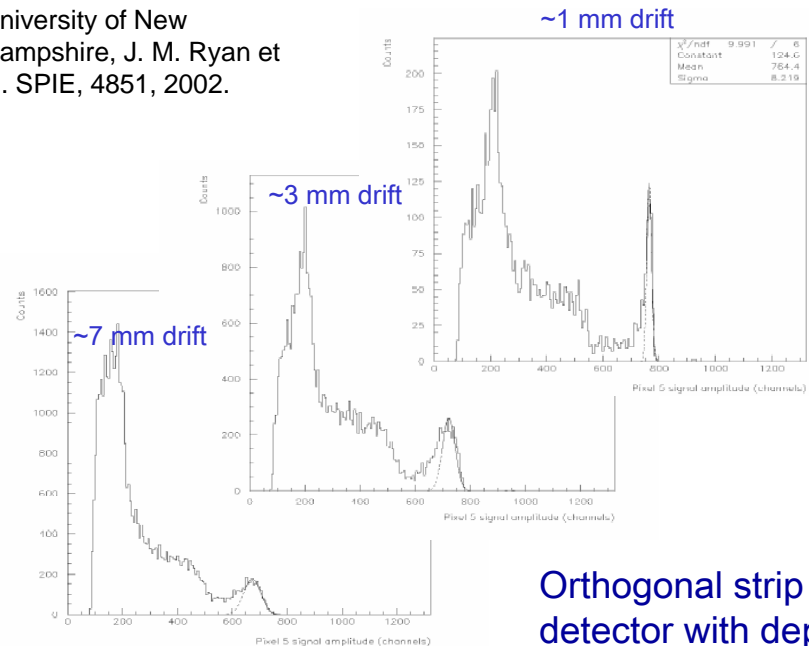
Statistical limit at 662 keV:  $\sim 4.3$  keV or  $\sim 0.7\%$  FWHM.

**Fano-factor for CZT is 0.089.**

“Semiconductors for Room-Temperature Radiation Detector Applications”, V. 487, p.217-222, 1997. eds. R.B. James, et. al.

2) Energy resolution degrades with electron drift distance.

University of New Hampshire, J. M. Ryan et al. SPIE, 4851, 2002.

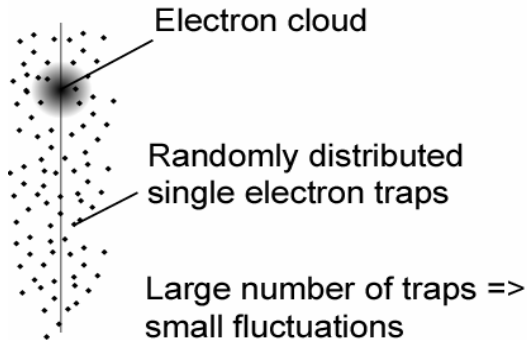


Orthogonal strip detector with depth sensing technique

To explain these results one must introduce additional source of fluctuations. The fact that energy resolution correlates with electron lifetime suggests that these fluctuations are caused by electron trapping process.

# Mechanism of charge loss fluctuations

## Case 1



If trapping centers are randomly distributed and each center traps a single electron then dispersion of lost charge  $D(N)$ :

$$D(N) = N$$

Relative fluctuation of collected charge:

$$\delta = \{D(N)\}^{1/2} / N_0 = N^{1/2} / N_0 < 1 / N_0^{1/2}$$

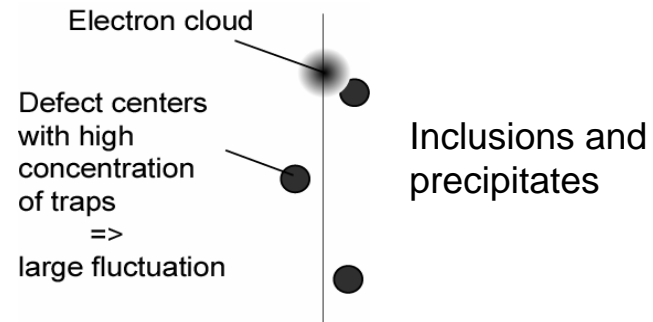
( $N_0$  total number of produced electrons)

For 662 keV photon produces  $N_0 \sim 1.3 \times 10^6$  electron-hole pairs.

$$< 0.1\%$$

Cannot explain observed fluctuations

## Case 2



Number of lost electrons:  $N = np$ ,  
 $p$  - average number of electrons trapped by a center  
 $n$  - average number centers encountered by electron cloud

If total charge loss is small, then,  $\varepsilon$  and  $n$  are independent

$$D(N) = D(p)n^2 + D(n)p^2$$

$D(\varepsilon)$  and  $D(n)$  are dispersions of  $\varepsilon$  and  $n$ . As a first approximation  $D(n) \cong n$ ,  $D(p) \cong p$ , then

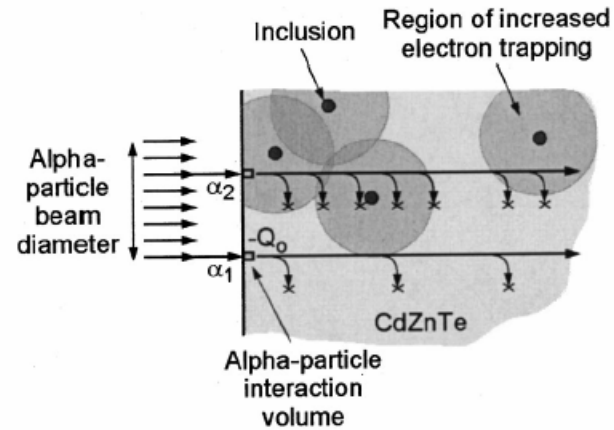
$$D(N) \cong pn^2 + np^2$$

$$\text{If } p/n < 10 \Rightarrow FWHM = 2.36np^{1/2}.$$

Fluctuations is proportional to the total number of defect centers encountered by electron cloud as it drifts toward anode.

## Electron trapping nonuniformity

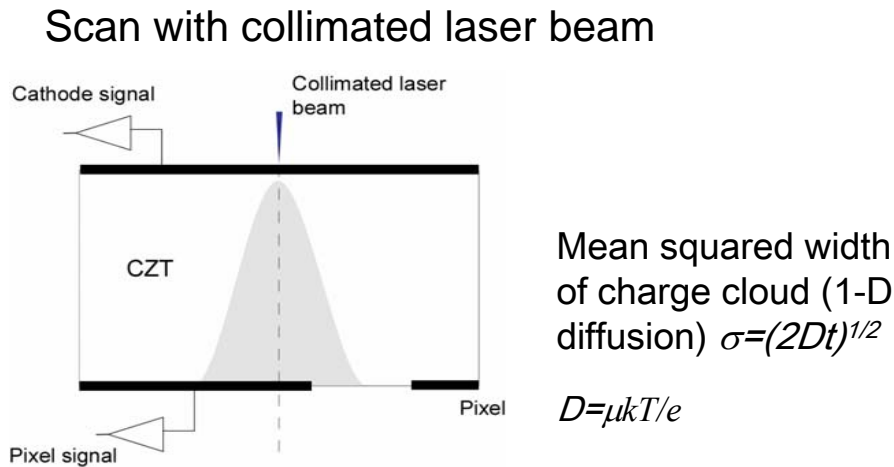
LBNL results (M. Amman, J. S. Lee,  
and P. N. Luke, J. App. Phys. 92, n. 6,  
p. 3198, 2002)



Fluctuations are due to different  
locations of interaction points

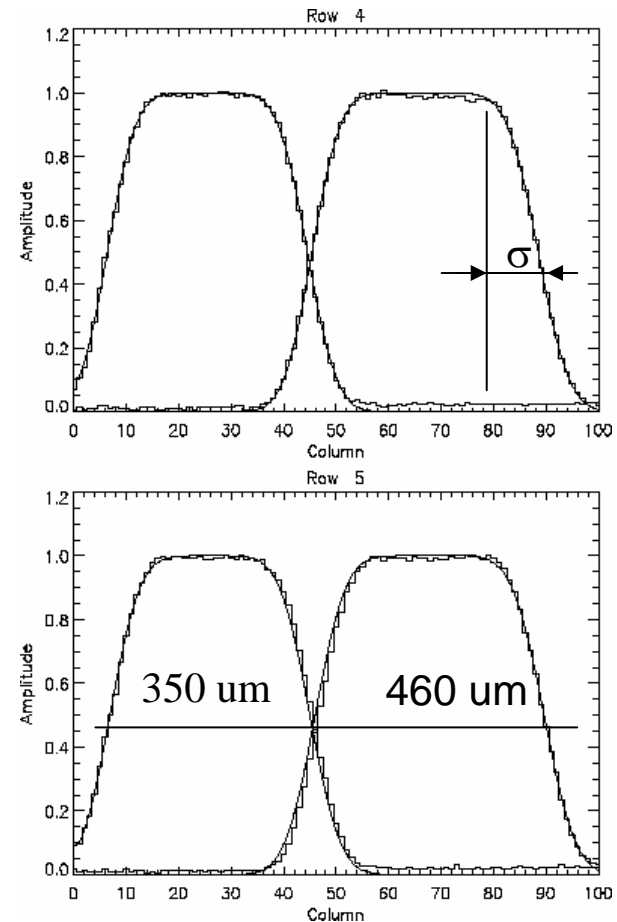
## Microscopic defects may explain large diffusion in CZT

Measured diffusion coefficient in CZT was found to be significantly larger than calculated based on Einstein equation.



Fitting edges with Error function gave  
 $D = 50-60 \text{ cm}^2/\text{s}$

Calculated based on Einstein equation  
gives  $D = 25 \text{ cm}^2/\text{s}$



Caltech, HEFT data

## Conclusions to fluctuation of electron losses

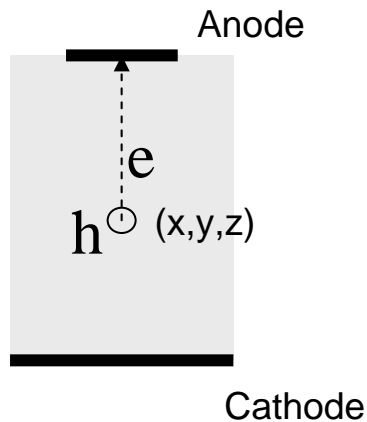
Charge loss fluctuations:

- set limit on energy resolution of current CZT devices (intrinsic resolution) which far above a statistical limit
- these fluctuations cannot be corrected as it can be done in the case of “continues” charge lose

To minimize this problem higher quality CZT crystals are required.

### III. Effects related to detector geometry

Most of detector designs were introduced to overcome poor hole collection



Electrons are collected.

Holes don't move (trapped instantly)

$$A_{\text{out}} = Q_e - Q_{\text{induced}}(x,y,z) \Rightarrow$$

$$A_{\text{out}} = f(x,y,z)$$

#### Variety CZT devices

Pixel

Coplanar-grid (P. Luke)

Virtual Frisch-grid

} to be discussed here

Strip

Drift-strip

Orthogonal Coplanar Anode Strip

Hemispherical

Three-electrode

Intelligent (Zhong He)

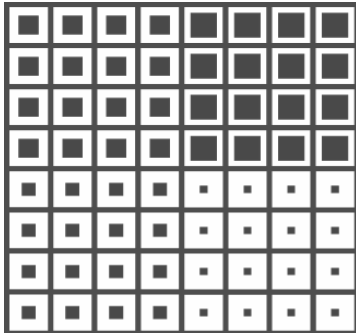
Coplanar-pixel

Cluster pixel

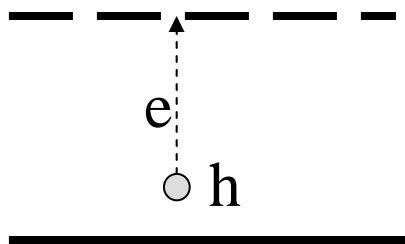
All these designs came from gas detectors: wires, pads, microstrip, TPC, etc. chambers

# Pixel detectors

Example of pixel contact pattern

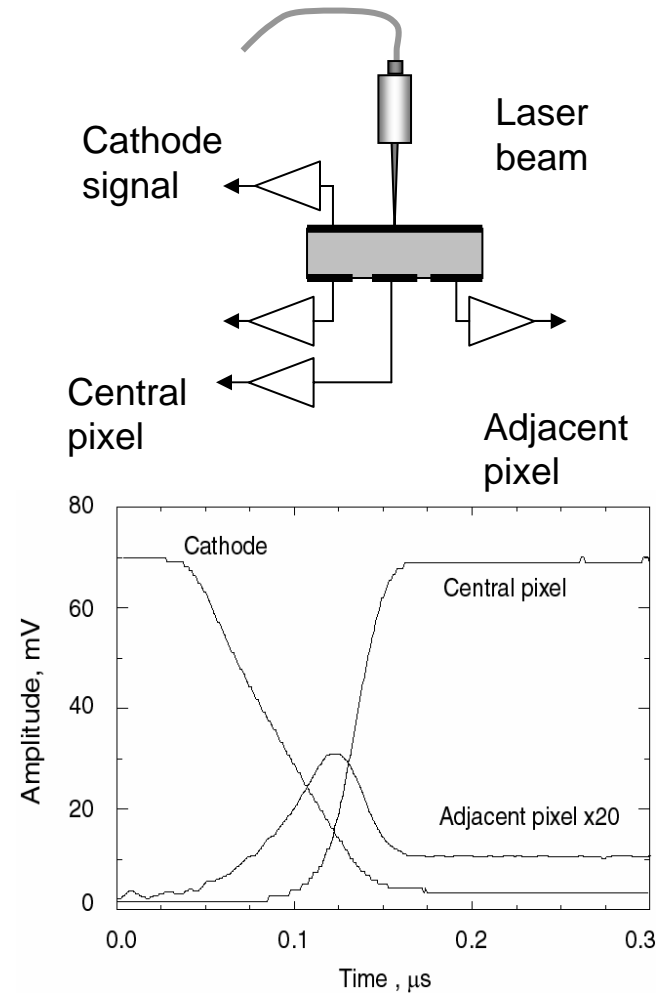


“Small pixel” effect



$$A_{\text{out}} = Q_e - Q_{\text{induced}}$$

$$Q_{\text{induced}} \sim 1/N$$

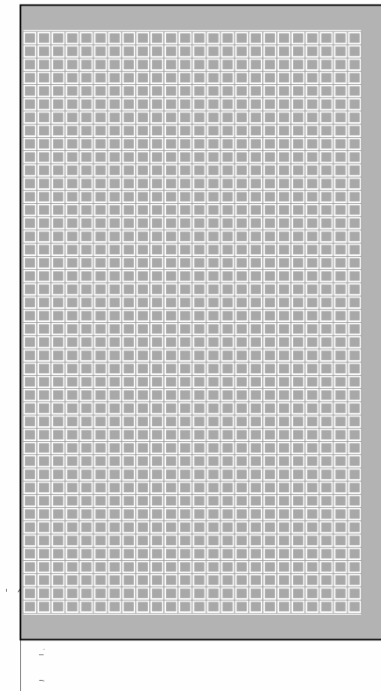
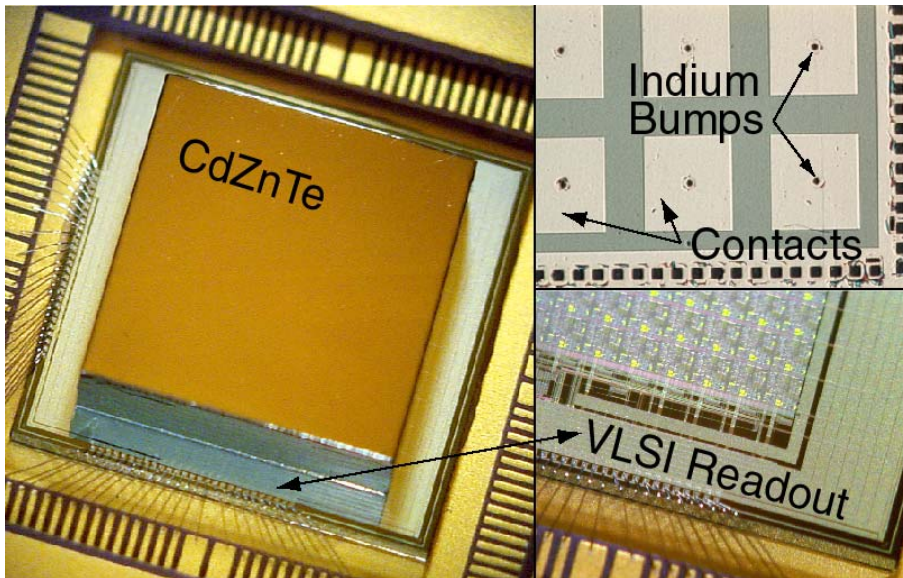


## Example of pixel device

### High Energy X-ray Focusing Telescope (HEFT), Caltech

- two 13x24x2 mm CZT pixel detectors indium-bump bonded to 24x48 channel ASIC
- pitch 500x500  $\mu\text{m}$ ,
- energy range 10-100 keV
- energy resolution < 1 keV
- CZT detectors are fabricated by eV-Products, Inc.

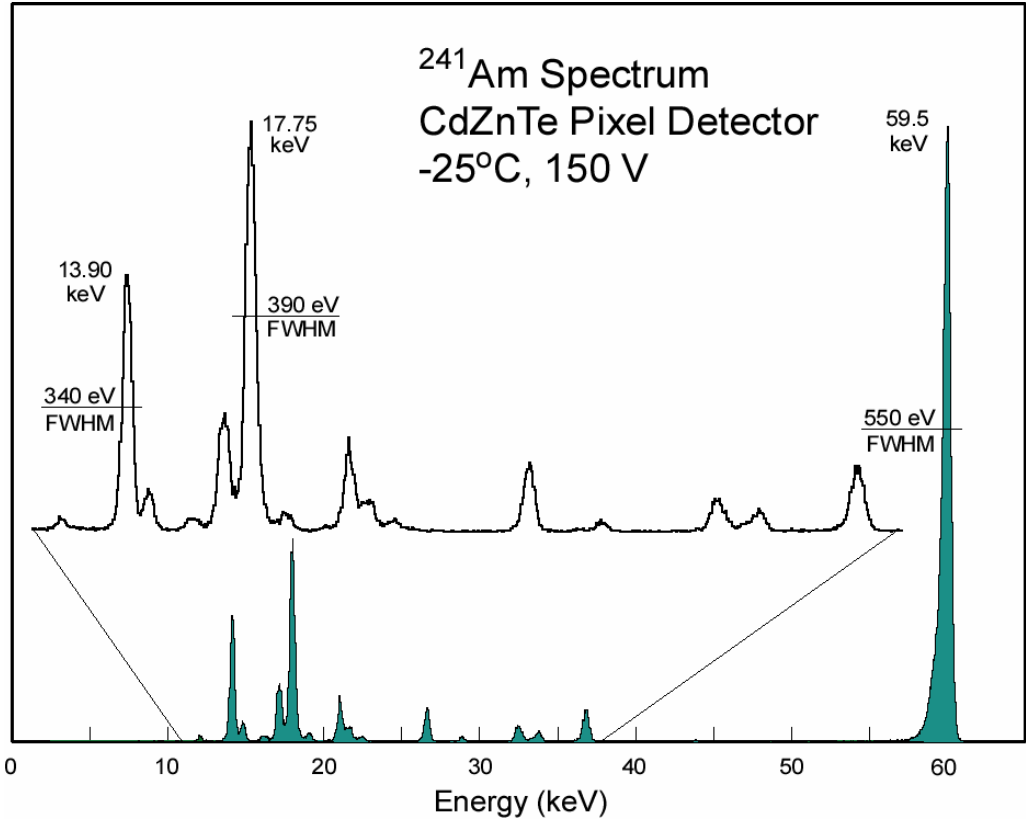
#### CZT/VLSI hybrid prototype



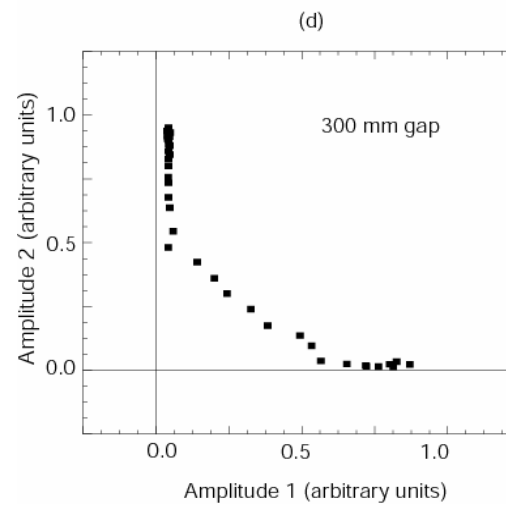
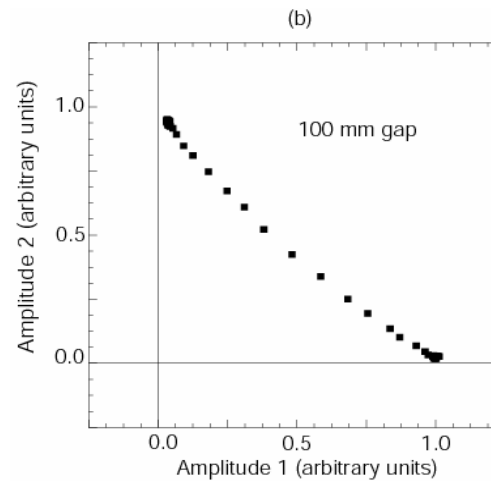
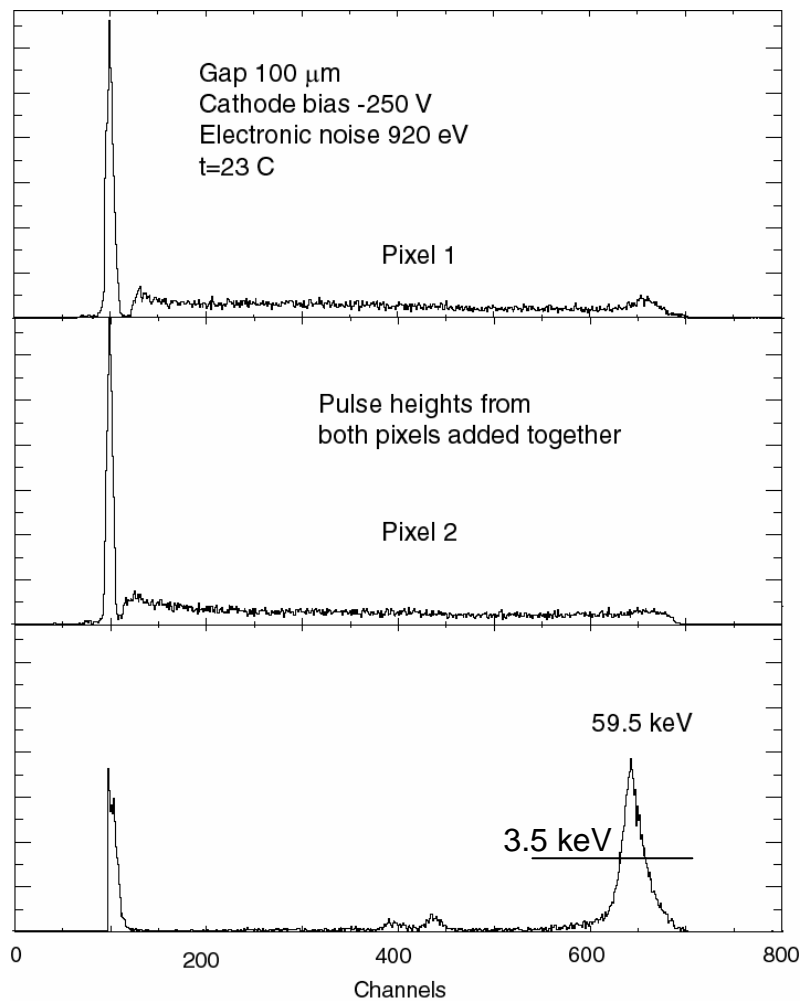
12x22 mm contact pattern  
13x24 mm CZT  
13x26 mm VLSI

Energy resolution on pixel device

Caltech, HEFT

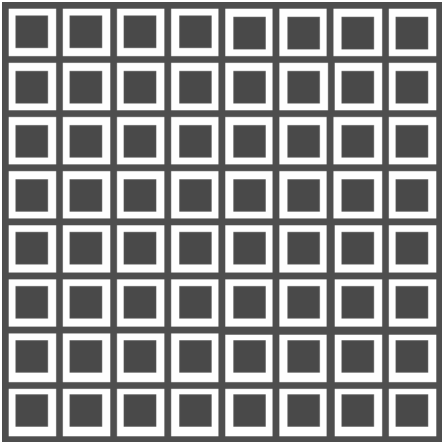
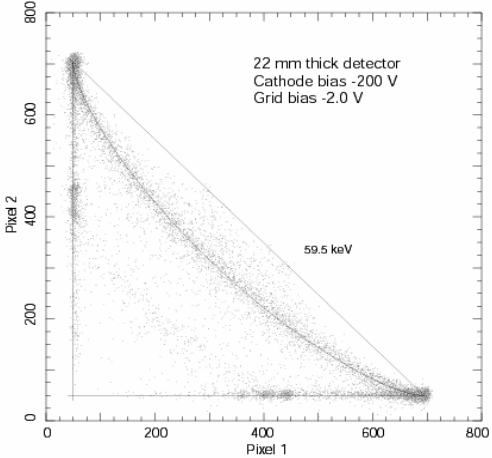


## Charge sharing between adjacent pixels

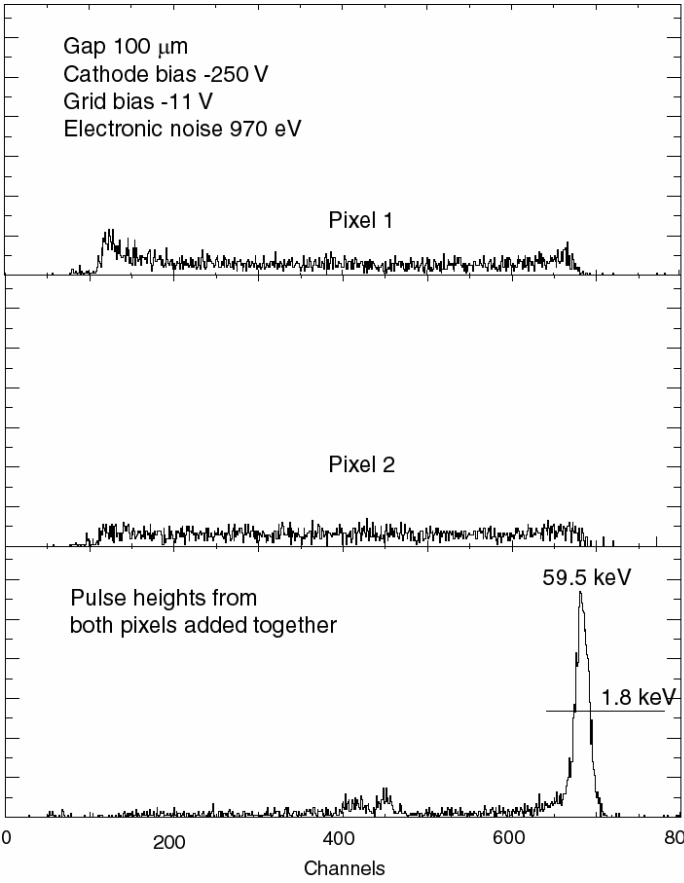
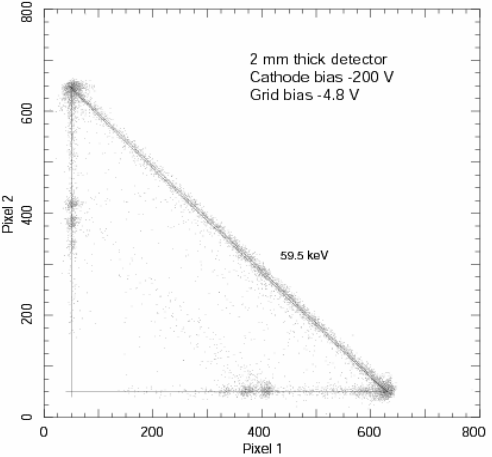


# Use of steering grid or very small gaps between pixels

(b)



(d)



Pattern with grid

## Cluster-pixel device

Main advantage of this device: small contact size of pixel =>

- low capacitor, low noise, excellent energy resolution, potentially approaching statistical limit

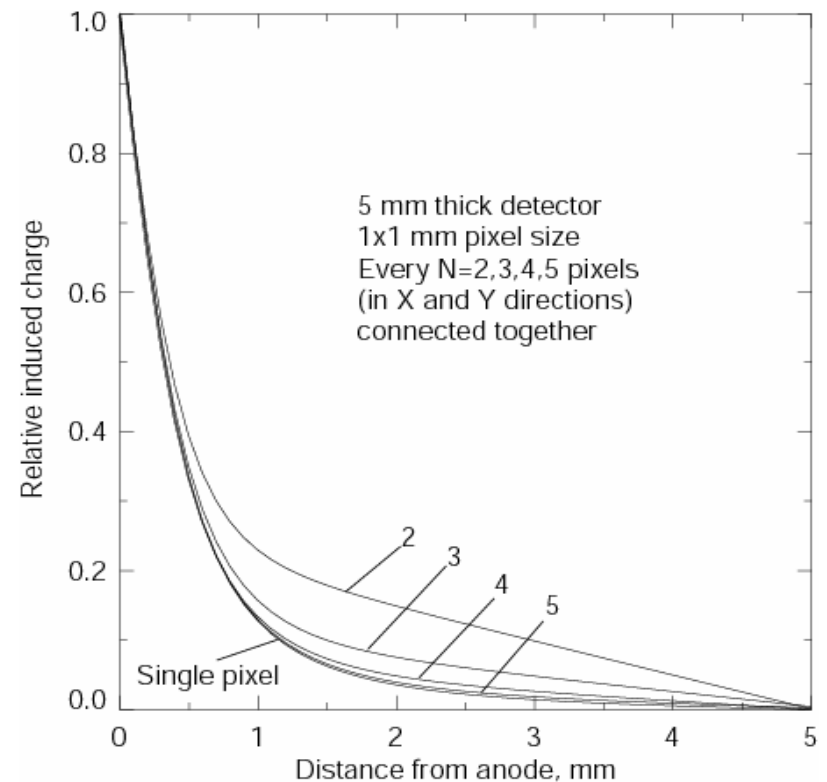
- capability reject "bad" area of CZT

- imaging, smallest pitch ~ 400  $\mu\text{m}$

- however, it requires ASIC

If position sensitivity is not required it is possible to group pixels

- Connecting every fourth pixel doesn't reduce significantly "small pixel effect", but significantly reduce a number of readout channels: 16!



## Coplanar-grid device

Miroshnichenko, B.U. Rodionov, and E. Shuvalova,  
 "Method of detection of gamma quanta", USSR patent  
 SU-1264723A, issued on June 15, 1986

P. Luke, 1994

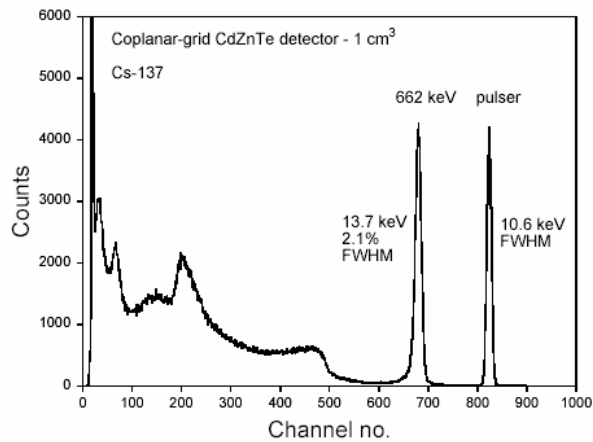
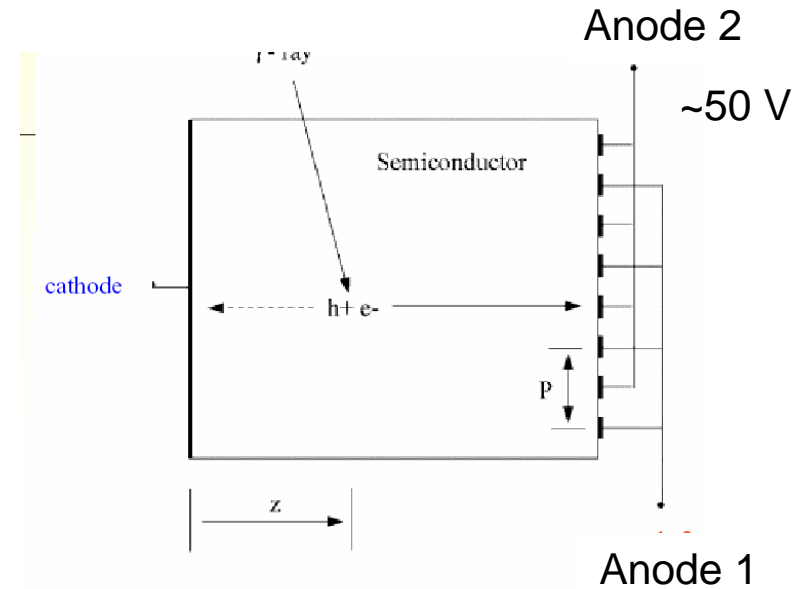
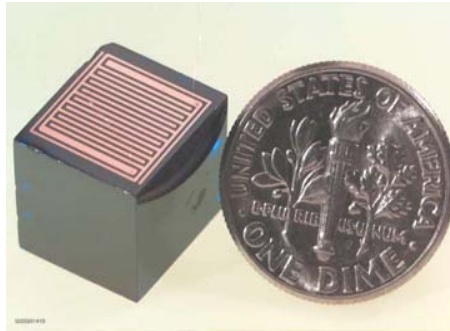


Fig. 1. A spectrum obtained from a Cs-137 gamma-ray source using a 1-cm<sup>3</sup> coplanar-grid CdZnTe detector.

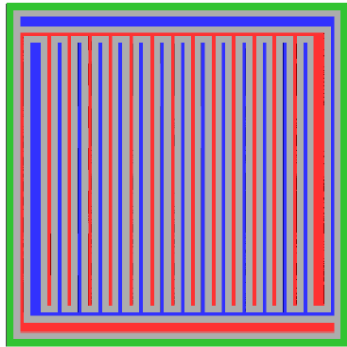
$$A_1 = Q_e - Q_{\text{induced}}$$

$$A_2 = -Q_{\text{induced}}$$

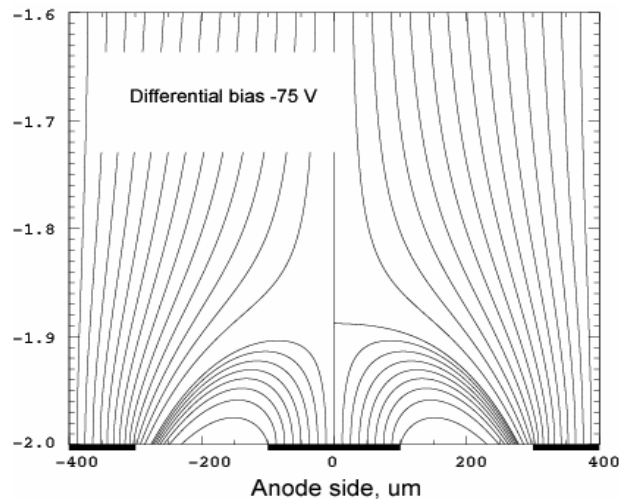
( $Q_{\text{induced}}$  is the same for both sets of electrodes).

$$A = A_1 - A_2 = Q_e$$

## Coplanar-grid device performance



Differential bias 75 V

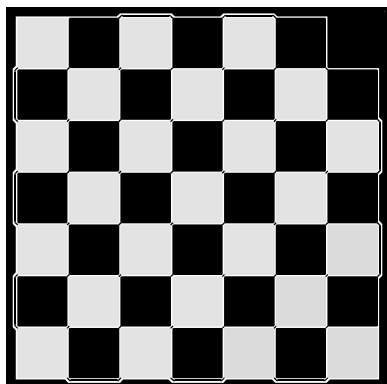


Drawbacks of coplanar-grid detectors:

- required differential bias between strips
- charge losses near the surface between strips
- grid pattern is not symmetrical => non-uniform response
- high surface leakage current but... electronic noise due to surface current is low (space-charge limited current)

Theoretically, it allows very good energy resolution. However, statistical limit was never achieved!

## Coplanar-pixel device

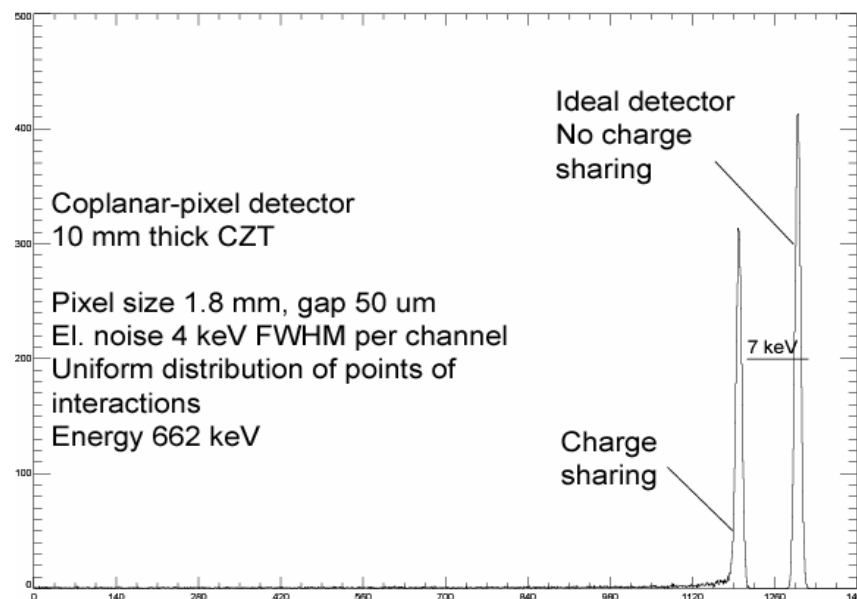


Coplanar-pixels mask  
BNL-05-16-03  
Preliminary drawing  
Size 11.8x11.8 mm

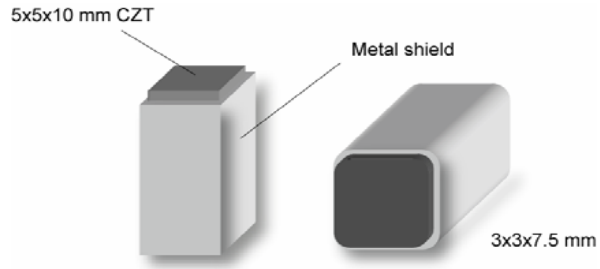


### Coplanar-pixels pattern

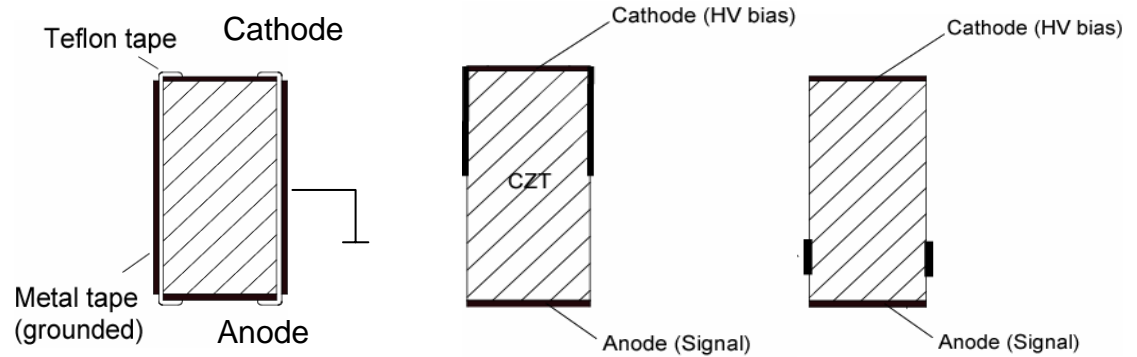
- contact pattern become symmetrical => uniform response
- pixel size is large
- no differential bias is needed => no surface leakage current



# Virtual Frisch-grid device



Virtual-grid detector array



$$A_{out} = Q_e - Q_{induced}$$

$$Q_{induced} \sim 0$$

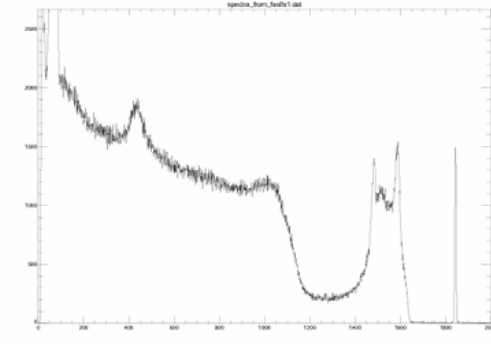
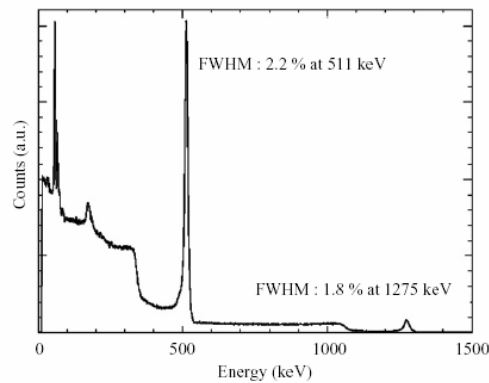
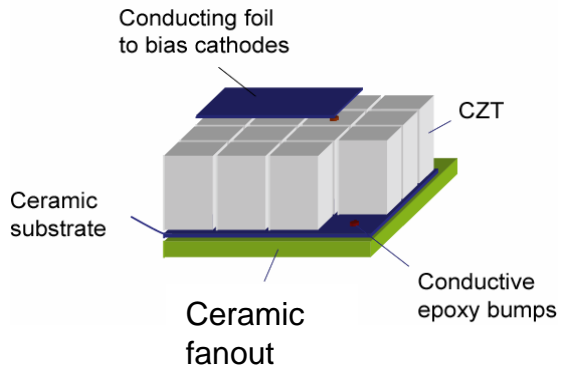
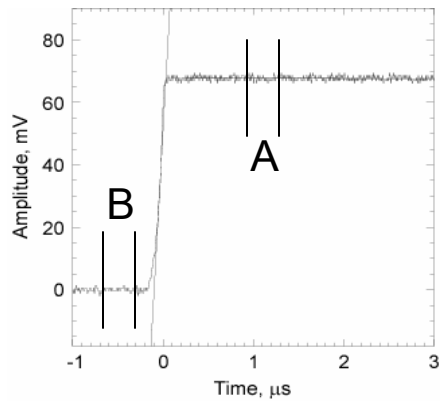


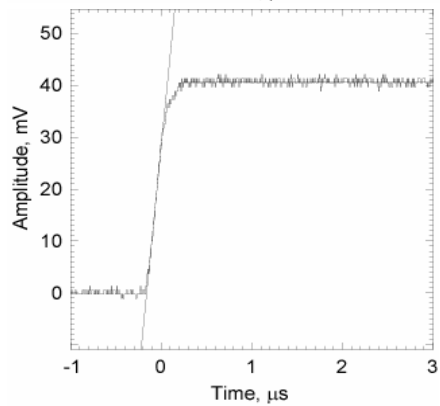
Fig. 13. <sup>22</sup>Na spectrum recorded with a 6 mm thick CZT Capacitive Frisch Grid Structure at 21°C, 400V.

## Digital pulse shaping and pulse rejection

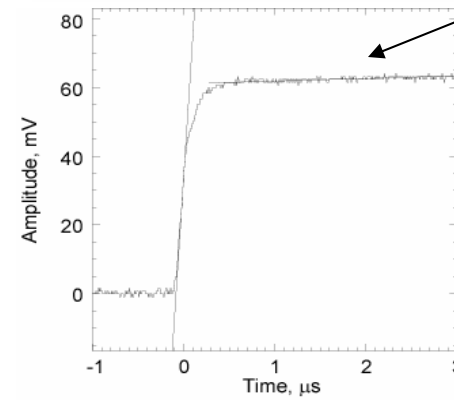
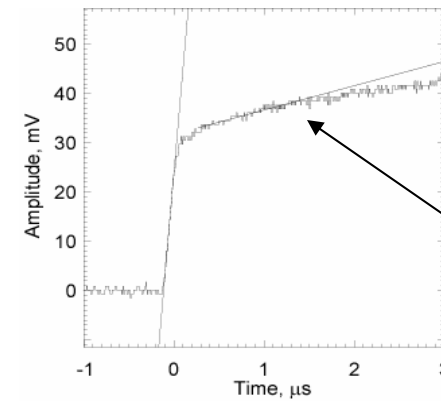
Example of accepted events



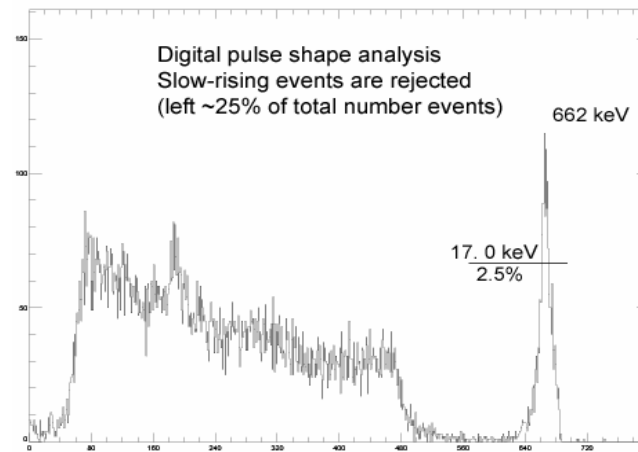
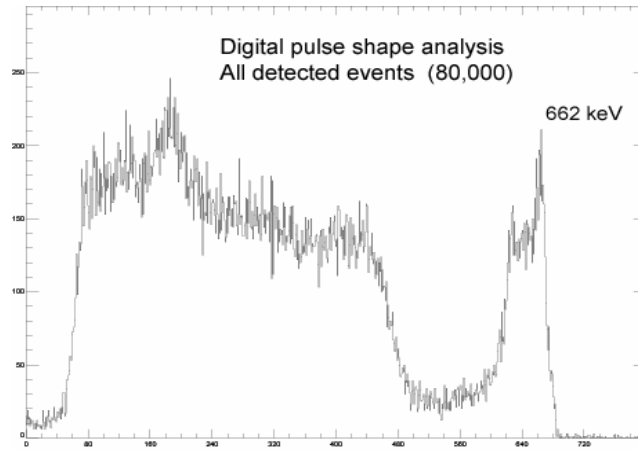
$$\text{Amp} = \sum A(i) - \sum B(i)$$



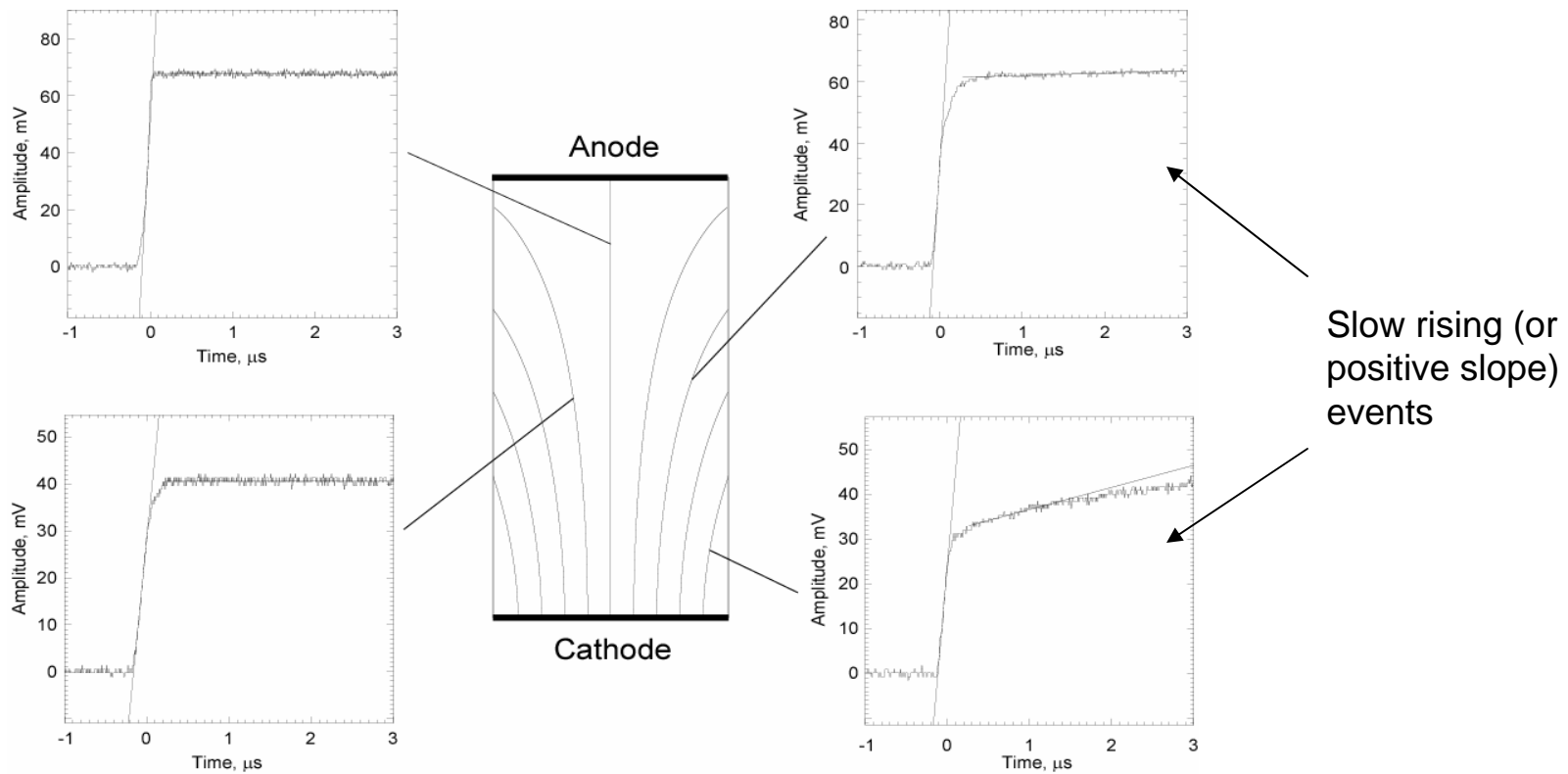
Example of rejected events



## Digital shaping and pulse rejection (Bar detector)



## Field defocusing effect in bar detectors



Electron mobility is slow near CZT surface due to scattering

## Conclusion

Most of the problems described here would be eliminated if material properties of CZT were better.

Improvements in CZT crystal growth are clearly needed!

## Schottky barrier models

Historically, two barrier models were proposed: **diffusion** and **thermionic-emission**. Both models give same “diode-like” expression for current across a barrier:

$$I = I_{SAT}(exp(eV/kT)-1), I = I_{SAT} \text{ (in reverse case)}$$

but expressions for **saturation current**,  $I_{SAT}$ , are different. Later, these models were combined together in so-called generalized thermionic-diffusion model developed by Sze.

**Diffusion** and **thermionic** models represent to limiting case of equilibrium condition at metal-semiconductor interface.

### Diffusion-limited case (“slow” semiconductors)

Carrier mobility is not sufficiently high to break thermal equilibrium at MS interface => carrier concentration at the surface is constant

$$I_{SAT} = e\mu EN = e\mu EN_0 \exp(-eV_{bi}/kT)$$

In reverse case, it depends on depletion and applied bias

### Thermionic-limited case (fast semiconductors, Si, Ge)

Mobility is very high; free carriers are removed immediately from interface => current is determined by the rate thermal emission over barrier

$$I_{SAT} = AT^2 \exp(-eV_0/kT)$$

Specific temperature dependence

**Generalized model doesn't give analytic expression for current!**

# Electron lifetime measurements

